phys. stat. sol. (b) **241**, No. 14, 3311–3317 (2004) / **DOI** 10.1002/pssb.200405225

Hydrostatic pressure effects on the donor impurity-related photoionization cross-section in cylindrical-shaped GaAs/GaAlAs quantum well wires

J. D. Correa[1], **O. Cepeda-Giraldo**[2], **N. Porras-Montenegro**[3], and **C. A. Duque**[*, 1]

[1] Instituto de Física, Universidad de Antioquia, AA 1226, Medellín, Colombia
[2] Departamento de Ciencia Básica, Universidad de Medellín, AA 1983, Medellín, Colombia
[3] Departamento de Física, Universidad del Valle, AA 25360, Cali, Colombia

Received 25 June 2004, revised 2 September 2004, accepted 2 September 2004
Published online 27 October 2004

PACS 62.50.+p, 71.55.Eq, 73.21.La, 78.67.He

Using a variational method the binding energy has been calculated for a shallow donor impurity and the donor-related photoionization cross-section in 1D and 0D GaAs low-dimensional systems. The dependence on the binding energy and the photoionization cross-section for a hydrogenic donor impurity in the finite potential model are discussed and the results are presented as a function of the radius, polarization of the photon, applied hydrostatic pressure, and photon energy. The calculations for the pressure effects are performed both in the direct and indirect GaAs gap regime. Calculations are presented for an on-axis (on-center) impurity in the wire (in the dot).

1 Introduction

The study of low-dimensional systems in the last few years has been very productive from the theoretical and experimental point of view. Optical properties associated with shallow donor impurities have attracted particular interest. One property of great interest is the impurity-related photoionization cross-section. Theoretical studies on the impurity position and dot/wire size-dependent binding energy in spherical quantum dots (QDs) and cylindrical quantum well wires (QWWs) have been reported [1, 2]. Porras-Montenegro and Pérez-Merchancano [1] have calculated the binding energy of donor/acceptor impurities in QDs, showing that the binding energy increases as the dot radius decreases up to a maximum and then decreases. Brown and Spector [3] calculated the impurity binding energy, using an infinite and a finite cylindrical confining potential, for both on-axis and off-axis impurities in QWWs.

The hydrostatic pressure effects on the electronic and impurity states in low-dimensional heterostructures such as quantum wells, QWWs, and QDs have been studied in several theoretical works [4–9]. Elabsy [4] has calculated the effects of the hydrostatic pressure on the binding energy of donor impurities in quantum well heterostructures, finding that the binding energy increases with increasing external hydrostatic pressure for a given quantum well thickness and temperature. Oyoko et al. [9] have studied the effects of a uniaxial stress on the binding energy of shallow donor impurities in parallelepiped-shaped GaAs/GaAlAs QDs. They have found that the binding energy increases almost linearly with applied stress and diminishes with the sizes of the structure. Correa et al. [10] have calculated the effects of hydrostatic pressure on the binding energy and photoionization cross-section in spherical QDs for different dimensions of the structure and radial impurity position. They have shown that the binding energy and

[*] Corresponding author: e-mail: cduque@fisica.udea.edu.co

photoionization cross-section are affected by the pressure. Also, they have shown that the photoionization cross-section is dominated by the behavior of the binding energy.

Sali et al. [11] have calculated the photon energy dependence of the donor impurity-related photoionization cross-section in rectangular QDs, in the infinite confinement potential model, as a function of the size of the dot and the impurity position. They have shown that the photoionization cross-section is greatly dependent on the size of the dot and the impurity position. Using a variational procedure, Ham and Spector [12] have calculated the photoionization cross-section for hydrogenic impurities in spherical QDs taking into account the energy and polarization of the photon. They found that for on-center impurities the transitions take place between the impurity level associated with the ground subband and the free particle state in the second subband. The cross-section is independent of the polarization of the photons. Additionally, for off-center impurities the transitions take place between the impurity level associated with the ground subband and the ground subband free particle state when the photons are polarized along the direction connecting the impurity with the center of the dot. Ham and Lee [13] have calculated the photoionization cross-section related to on-axis hydrogenic impurities in cylindrical QWWs. They found that the photoionization cross-section increases with increasing wire size, reaching a maximum value and then decreasing with a further increase in wire size.

In the present paper, using a finite confinement potential model and the variational method, we calculate the photoionization cross-section for a shallow donor impurity in cylindrical GaAs/GaAlAs QWWs under hydrostatic pressure effects. The size of the structure and the photon energy are also considered. Additionally, for the purpose of analyzing the reduction of the dimensionality of the system, we present some results for the photoionization cross-section related to on-center impurities in GaAs/GaAlAs QDs.

2 Theoretical framework

The Hamiltonian, in the effective-mass approximation, for on-axis hydrogenic shallow donor impurities in a cylindrical QWW is

$$H = -\frac{\hbar^2}{2}\nabla\cdot\left(\frac{1}{m^*_{w,b}(P)}\nabla\right) - \frac{e^2}{\varepsilon_{w,b}(P)\sqrt{\rho^2+z^2}} + V(\rho,P) \tag{1}$$

where $V(\rho, P)$ is the finite confinement potential [4].

The eigenfunctions of the Hamiltonian in Eq. (1) in the absence of the impurity potential are

$$\psi(\rho,z) = N\left[\Theta(R-\rho)\,J_0(k_1\rho)\,\mathrm{e}^{-\mathrm{i}kz} + \Theta(\rho-R)\frac{J_0(k_1 d)}{K_0(k_2 d)}K_0(k_2\rho)\,\mathrm{e}^{-\mathrm{i}kz}\right] \tag{2}$$

where $\Theta(x)$ is the usual step function, N is the normalization constant, and R is the radius of the cylindrical QWW. The inclusion of the impurity forces the use of the variational approach. When the impurity is located along the axis of the wire, the trial wave function for the 1s-like ground state is given by

$$\psi(\rho,z) = M\left[\Theta(R-\rho)\,J_0(k_1\rho)\,\mathrm{e}^{-\lambda\sqrt{\rho^2+z^2}} + \Theta(\rho-R)\frac{J_0(k_1 R)}{K_0(k_2 R)}K_0(k_2\rho)\,\mathrm{e}^{-\lambda\sqrt{\rho^2+z^2}}\right] \tag{3}$$

where M is the normalization constant and λ is the variational parameter. In Eqs. (2) and (3) $J_n(x)$ and $K_n(x)$ are the Bessel function and the modified Bessel function, respectively [2].

The binding energy is calculated from the difference between the eigenvalue in Eq. (1) without the impurity potential term and the eigenvalue associated with the wave function in Eq. (3) minimized with respect to the variational parameter λ [9].

The eigenfunction for the spherical QD in the finite confinement potential model, without the impurity, is

$$\psi_{l,m}(r,\theta,\phi) = N'\left[\Theta(R-r)\;j_l(\xi_{1l}r)\,Y^l_m(\theta,\phi) + \Theta(r-R)\frac{j_l(\xi_{1l}R)\,\mathrm{e}^{\chi_{1l}(R)R-\chi_{1l}(r)r}}{r}Y^l_m(\theta,\phi)\right] \tag{4}$$

and in the presence of an on-center impurity the trial wave function is

$$\Psi_{l,m}(r,\theta,\phi) = M'\psi_{l,m}(r,\theta,\phi)\,\mathrm{e}^{-\lambda|r|}\,. \tag{5}$$

In Eqs. (4) and (5) $j_l(\xi_{1l}r)$ is the spherical Bessel function, $Y_m^l(\theta,\phi)$ is the spherical harmonic, and λ is the variational parameter [1].

The photoionization cross-section is given by [11]

$$\sigma(\hbar w) = \left[\left(\frac{\zeta_{\mathrm{eff}}}{\zeta_0}\right)^2 \frac{n}{\varepsilon_{\mathrm{d}}(P)}\right]\frac{4\pi^2}{3}\alpha_{\mathrm{FS}}\hbar w\sum_f \left|\left\langle\Psi_f\left|r\right|\Psi_i\right\rangle\right|^2\delta(E_f - E_i - \hbar w) \tag{6}$$

where n is the refraction index of the semiconductor, α_{FS} is the fine structure constant, $\hbar w$ is the photon energy, $\zeta_{\mathrm{eff}}/\zeta_0$ is the ratio of the effective electric field of the incoming photon to the average electric field in the medium, and $\langle\psi_f|r|\psi_i\rangle$ is the matrix element of the dipole moment of the impurity.

For on-axis impurities in cylindrical QWWs the final and initial states are those from Eqs. (2) and (3), respectively. In the effective-mass approximation the donor-related photoionization cross-section in QWWs is given by

$$\sigma(\hbar w) = \left[\left(\frac{\zeta_{\mathrm{eff}}}{\zeta_0}\right)^2 \frac{n}{\varepsilon_{\mathrm{d}}(P)}\right]\frac{2\pi}{3}\alpha_{\mathrm{FS}}\hbar w(\hbar w - E_{\mathrm{b}})^{1/2}N^2M^2 4\pi^2 d^5 H_1 a_0^2 \tag{7}$$

where

$$H_1 = \frac{4d^3}{(\lambda^2+x)^2}I_1^2 + \frac{16d^2}{(\lambda^2+x)^{5/2}}I_1I_2 + \frac{16d}{(\lambda^2+x)^3}I_2^2 \tag{8}$$

with

$$I_1 = \int_0^\infty \mathrm{d}t\; t^3\varphi^2(t)K_0(tR\sqrt{\lambda^2+x}) \tag{9}$$

and

$$I_2 = \int_0^\infty \mathrm{d}t\; t^2\varphi^2(t)\,K_1(tR\sqrt{\lambda^2+x})\,. \tag{10}$$

In Eqs. (9) and (10)

$$\varphi(t) = \Theta(t-1)\,J_0(k_1Rt) + \Theta(1-t)\frac{J_0(k_1R)}{K_0(k_2R)}K_0(k_2Rt) \tag{11}$$

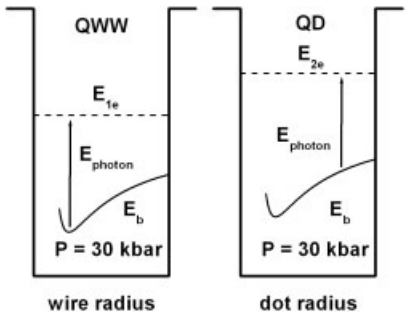

Fig. 1 Schematic representation of the fundamental well states of the electron in the QWW and the first excited state in the QD (dashed lines). Solid lines correspond to the donor impurity binding energies. Arrows indicate the photon energy used in the photoionization cross-section.

with

$$x = \hbar w - E_b(P) \tag{12}$$

where $E_b(P)$ is the pressure-dependent binding energy.

Figure 1 shows the selection rules for the photoinization cross-section associated with on-axis and on-center impurities in the transverse section of the wire and in the volume of the dot, respectively.

The details of the pressure-dependent Hamiltonian, binding energy, and donor-related photoionization cross-section for a shallow donor impurity in spherical QDs are given in Ref. [10].

3 Results and discussion

In agreement with previous experimental work [14, 15] it is clear that the potential that confines the electrons in the whole range of the applied pressures is essentially given by the difference between the energy associated with the Γ point in the conduction band for the barrier material and the well material. However, the Γ–X crossing in the barrier material for pressure values close to 13.5 kbar generates an interference in the height of the potential well, and as a consequence there is a deviation of the linear behavior for the hydrostatic pressure of the photoluminescence spectra (see, for example, the high-pressure range in Fig. 5a of Ref. [14]). Burnett et al. [15] have calculated the confined electron states in single and double GaAs/GaAlAs quantum wells including the Γ–X mixing in the two-band Hamiltonian for electrons in order to describe the non-linear behavior with pressure in the photoluminescence spectra. In the present work we follow the Elabsy model [4] for the potential barrier that confines the electrons in the QD and in the QWW. In this one-band qualitative model [4], which shows very good agreement with the experimental results, the pressure dependence of the QD and QWW parameters are characterized by the following: (i) the electron conduction mass in the well and in the barrier increases linearly with pressure; (ii) the dielectric constant in the well and barrier decreases linearly with pressure; (iii) the volume change in the zinc-blend structure under hydrostatic pressure produces a linear reduction of the QD and QWW radius; and (iv) the barrier height does not change in the range 0–13.5 kbar and for higher pressures it decreases to zero at 33.5 kbar.

Figure 2 shows the results for the binding energy as a function of the wire/dot radius for different values of the hydrostatic pressure. Due to the 3D confinement in the QD, the potential barrier effect on the electron wave function is larger than that for the QWW, where the confinement is 2D type. For this reason, the expected value of the electron–impurity separation is smaller and the binding energy is larger in the QD case than in the QWW case for each value of the pressure. One of the fundamental effects of the pressure is the reduction of the potential barrier height, which facilitates the penetration of the electron wave functions into the barrier region. This is manifested in a decrease of the binding energy, just as can be seen when comparing curves 1, 2, and 3 in Figs. 2a and b.

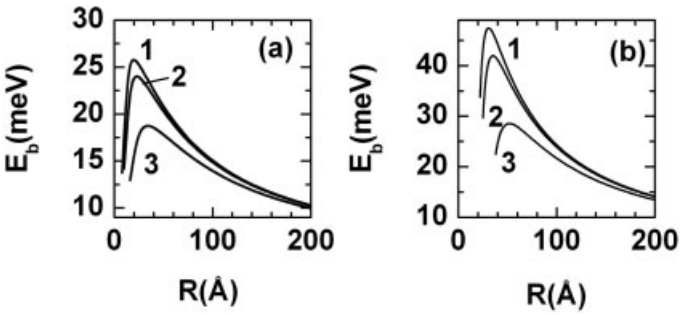

Fig. 2 Binding energy of a shallow donor impurity as a function of the radius of a) cylindrical GaAs-$Ga_{0.7}Al_{0.3}As$ QWW and b) spherical GaAs-$Ga_{0.7}Al_{0.3}As$ QD for various values of the hydrostatic pressure: $P = 0$ (curve 1), $P = 20$ kbar (curve 2), and $P = 30$ kbar (curve 3).

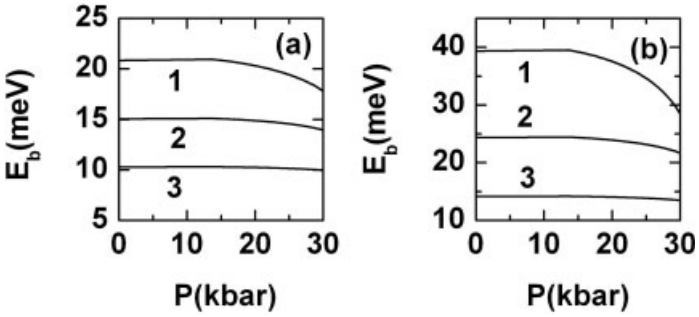

Fig. 3 Binding energy of a shallow donor impurity as a function of hydrostatic pressure for a) cylindrical GaAs-$Ga_{0.7}Al_{0.3}As$ QWW and b) spherical GaAs-$Ga_{0.7}Al_{0.3}As$ QD for different values of the radius of the structure: R = 50 Å (curve 1), R = 100 Å (curve 2), and R = 200 Å (curve 3).

Figure 3 shows the results for the binding energy as a function of the hydrostatic pressure for a cylindrical QWW and a spherical QD. In the direct gap regime (pressures less than 13.5 kbar) the small variations of the binding energy are associated with the pressure-dependent effective mass, dielectric constant, and radius of the wire/dot. For pressures higher than 13.5 kbar, for which the barrier height decreases, the wave function penetrates into the barrier region, increasing the electron–impurity separation and consequently decreasing the binding energy. The decrease of the binding energy with increasing radius of the structure (as one can see when comparing curves 1, 2, and 3 in Figs. 3a and b is consistent with the results presented in Fig. 2.

Figure 4 shows the photoionization cross-section of a shallow donor impurity as a function of the radius of the cylindrical QWW and spherical QD. In Fig. 4a, for each pressure curve, the photon energy corresponds to the maximum value of the binding energy in the corresponding curve in Fig. 2. In Fig. 4b the photon energy is obtained by means of $E_{2e} - E_{1e} + E_b$, where E_b is the impurity binding energy and E_{1e} and E_{2e} are the energies of the fundamental and first excited states of the electron in the QD. As the radius of the structure (wire/dot) grows the effects of the potential barrier on the electron wave function decrease, with and without the impurity potential. For this reason the wave functions of the initial state (impurity state) and final state (well state) are strongly symmetrical with respect to the axis/center of the structure. The overlap of the initial and final wave functions spreads to a maximum, giving a minimum in the value of the matrix element of the dipole moment of the impurity in Eq. (6). This effect is associated with the decrease in the photoionization cross-section with the radius of the structure in the two limits: in the limit of larger radius the wave functions are fundamentally located in the region of the well and they are symmetrical with respect to the axis/center, and in the limit of small radius the wave functions are essentially located in the region of the barrier. They are also strongly symmetrical with respect to the axis/center.

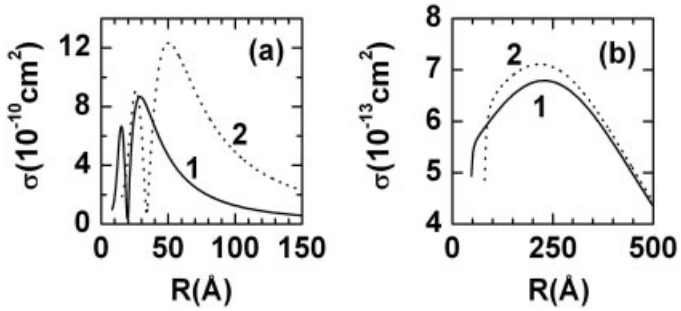

Fig. 4 Photoionization cross-section of a shallow donor impurity as a function of the radius of a) cylindrical GaAs-$Ga_{0.7}Al_{0.3}As$ QWW and b) spherical GaAs-$Ga_{0.7}Al_{0.3}As$ QD for two values of hydrostatic pressure: P = 0 (curve 1) and P = 30 kbar (curve 2).

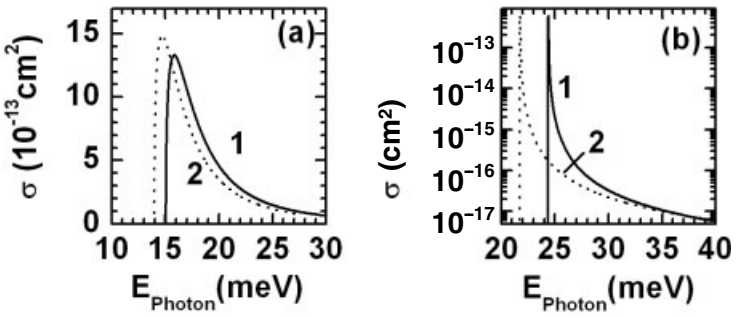

Fig. 5 Photoionization cross-section as a function of the photon energy of a shallow donor impurity in a) cylindrical GaAs-$Ga_{0.7}Al_{0.3}As$ QWW and b) spherical GaAs-$Ga_{0.7}Al_{0.3}As$ QD for R = 100 Å and two values of the hydrostatic pressure: P = 0 (curve 1) and P = 30 kbar (curve 2).

Figure 5 shows the results for the donor impurity-related photoionization cross-section as a function of the photon energy. Taking into account that for each pressure the matrix element of the dipole moment of the impurity and the binding energy are constant, the behavior of the curves is essentially due to the term associated with the incident photon in Eq. (6). The binding energy decreases with pressure due to the increase of the separation between the electron and the impurity, generating an increment in the matrix element of the dipole moment of the impurity. This effect creates the increment shown in curves 2 in comparison with curves 1. The increment in the incident photon energy generates a decrease in the probability of excitation of the final state in the well which corresponds to the asymptotic behavior in the photoionization cross-section curves.

4 Conclusions

Using a variational method for a hydrogenic donor impurity we have calculated the binding energy and the impurity-related photoionization cross-section in 1D and 0D GaAs low-dimensional systems. We have discussed the dependence on the binding energy and the photoionization cross-section for a hydrogenic donor impurity in the finite potential model and our results are presented as a function of the radius, the polarization of the photon, the applied hydrostatic pressure, and the photon energy. The calculations for the pressure effects are both in the direct and indirect GaAs gap regime. We have considered the different transition rules that depend on the impurity position and photon polarization. Calculations are presented for the impurity on-axis (on-center) in the wire (in the dot). We have found that the photoionization cross-section increases with the applied hydrostatic pressure. Additionally, we have observed that the photoionization cross-section increases or decreases depending on the photon polarization and radius of the wire/dot. We have shown that the photoionization cross-section decreases with the photon energy and that it is strongly affected by the size of the wire or the dot radius. The measurement of photoionization in such systems would be of great interest for understanding the optical properties of carriers in QWWs and QDs for which the photoionization can give information about the impurity position and distribution inside the structure.

A more realistic description of the problem should consider the convolution of the photoionization cross-section for randomly distributed impurities in the structures. Results for different transition rules that depend on the impurity position and photon polarization will be presented elsewhere. To the best of our knowledge, there are no experimental reports relating to the photoionization cross-section in semiconducting heterostructures such as quantum wells, QWWs, and QDs. We hope this work stimulates the development of measurements of the special impurity-related photoionization properties here presented in these kinds of systems.

Acknowledgements The authors are grateful to the Universidad de Antioquia-CODI for financial support. This work was partially financed by Colciencias, the Colombian Scientific Agencies, under grant numbers 1115-05-11502 and 1106-05-13828. The authors are grateful to N. Vanegas for a critical reading of the manuscript, and to U. Venkateswaran and M. Chandrasekhar for useful discussions.

Referenes

[1] N. Porras-Montenegro and S. T. Pérez-Merchancano, Phys. Rev. B **46**, 9780 (1992).
[2] N. Porras-Montenegro, S. T. Pérez-Merchancano, and A. Latgé, J. Appl. Phys. **74**, 7624 (1993).
[3] J. W. Brown and H. N. Spector, J. Appl. Phys. **59**, 1179 (1986).
[4] A. M. Elabsy, J. Phys. Condens. Matter **6**, 10025 (1994).
[5] A. L. Morales, A. Montes, S. Y. López, and C. A. Duque, J. Phys.: Condens. Matter **14**, 987 (2002).
[6] S. Y. López, N. Porras-Montenegro, and C. A. Duque, phys. stat. sol. (c) **0**, 648 (2003).
[7] A. L. Morales, A. Montes, S. Y. López, N. Raigoza, and C. A. Duque, phys. stat. sol. (c) **0**, 652 (2003).
[8] S. Y. López, N. Porras-Montenegro, and C. A. Duque, Semicond. Sci. Technol. **18**, 718 (2003).
[9] H. O. Oyoko, C. A. Duque, and N. Porras-Montenegro, J. Appl. Phys. **90**, 819 (2001).
[10] J. D. Correa, N. Porras-Montenegro, and C. A. Duque, phys. stat. sol. (b) **241**, 2440 (2004).
[11] A. Sali, H. Satori, M. Fliyou, and H. Loumrhari, phys. stat. sol. (b) **232**, 209 (2002).
[12] Heon Ham and H. N. Spector, J. Appl. Phys. **93**, 3900 (2003).
[13] Heon Ham and Cheol Jin Lee, J. Korean Phys. Soc. **42**, S286 (2003).
[14] U. Venkateswaran, M. Chandrasekhar, H. R. Chandrasekhar, B. A. Vojak, F. A. Chambers, and J. M. Meese, Phys. Rev. B **33**, 8416 (1986).
[15] J. H. Burnett, H. M. Cheong, W. Paul, E. S. Koteles, and B. Elman, Phys. Rev. B **47**, 1991 (1993).